

Muon $g - 2$ anomaly in a minimal left-right model with an inverse seesaw mechanism

Mustafa Ashry

mustafa@sci.cu.edu.eg

DEPARTMENT OF MATHEMATICS, FACULTY OF SCIENCE, CAIRO UNIVERSITY



Based on PhysRevD.107.055044 and PhysRevD.104.015016 [4, 10]
(In collaboration with *K. Ezzat* and *S. Khalil*)

The Dark Side of the Universe (DSU2023), Rwanda, 10-14 July 2023

Outline

1 The LRIS Model

2 a_μ in LRIS

3 LFV Constraints

4 Conclusion

Outline

1 The LRIS Model

2 a_μ in LRIS

3 LFV Constraints

4 Conclusion

Outline

1 The LRIS Model

2 a_μ in LRIS

3 LFV Constraints

4 Conclusion

Outline

- 1 The LRIS Model
- 2 a_μ in LRIS
- 3 LFV Constraints
- 4 Conclusion

Outline

1 The LRIS Model

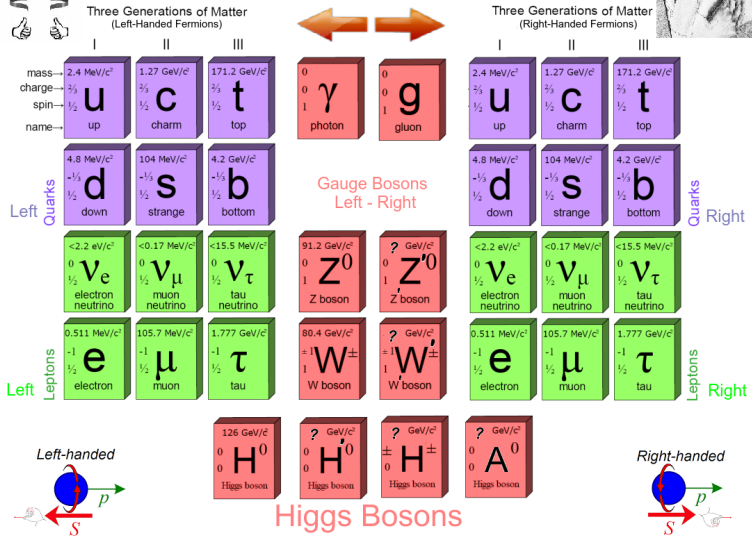
2 a_μ in LRIS

3 LFV Constraints

4 Conclusion



Left-Right Symmetric Model



Fields	$SU(3)_C \times SU(2)_L \times SU(2)_R \times U_{B-L}$	\mathbb{Z}_2
$Q_L = \begin{pmatrix} u_L \\ d_L \end{pmatrix}$	$(\mathbf{3}, \mathbf{2}, \mathbf{1}, \frac{1}{3})$	+1
$Q_R = \begin{pmatrix} u_R \\ d_R \end{pmatrix}$	$(\mathbf{3}, \mathbf{1}, \mathbf{2}, \frac{1}{3})$	+1
$L_L = \begin{pmatrix} \nu_L \\ e_L \end{pmatrix}$	$(\mathbf{1}, \mathbf{2}, \mathbf{1}, -1)$	+1
$L_R = \begin{pmatrix} \nu_R \\ e_R \end{pmatrix}$	$(\mathbf{1}, \mathbf{1}, \mathbf{2}, -1)$	+1
S_1	$(\mathbf{1}, \mathbf{1}, \mathbf{1}, -2)$	-1
S_2	$(\mathbf{1}, \mathbf{1}, \mathbf{1}, 2)$	+1
$\phi = \begin{pmatrix} \phi_1^0 & \phi_1^+ \\ \phi_2^- & \phi_2^0 \end{pmatrix}$	$(\mathbf{1}, \mathbf{2}, \mathbf{2}, 0)$	+1
$\chi_R = \begin{pmatrix} \chi_R^+ \\ \chi_R^0 \end{pmatrix}$	$(\mathbf{1}, \mathbf{1}, \mathbf{2}, 1)$	+1

Table 1: The LRIS particle Content quantum numbers.

- The Higgs potential is [6]

$$\begin{aligned}
 V(\phi, \chi_R) = & \mu_1 \text{Tr}(\phi^\dagger \phi) + \mu_2 [\text{Tr}(\tilde{\phi} \phi^\dagger) + \text{Tr}(\tilde{\phi}^\dagger \phi)] + \lambda_1 (\text{Tr}(\phi^\dagger \phi))^2 \\
 & + \lambda_2 [(\text{Tr}(\tilde{\phi} \phi^\dagger))^2 + (\text{Tr}(\tilde{\phi}^\dagger \phi))^2] + \lambda_3 \text{Tr}(\tilde{\phi} \phi^\dagger) \text{Tr}(\tilde{\phi}^\dagger \phi) \\
 & + \lambda_4 \text{Tr}(\phi \phi^\dagger) (\text{Tr}(\tilde{\phi} \phi^\dagger) + \text{Tr}(\tilde{\phi}^\dagger \phi)) + \mu_3 (\chi_R^\dagger \chi_R) + \rho_1 (\chi_R^\dagger \chi_R)^2 \\
 & + \alpha_1 \text{Tr}(\phi^\dagger \phi) (\chi_R^\dagger \chi_R) + \alpha_2 (\chi_R^\dagger \phi^\dagger \phi \chi_R) + \alpha_3 (\chi_R^\dagger \tilde{\phi}^\dagger \tilde{\phi} \chi_R) \\
 & + \alpha_4 (\chi_R^\dagger \phi^\dagger \tilde{\phi} \chi_R + h.c.). \tag{1}
 \end{aligned}$$

- The Yukawa Lagrangian

$$\begin{aligned}
 \mathcal{L}_Y = & \sum_{i,j=1}^3 \bar{L}_{L,i} (\phi y_{ij}^L + \tilde{\phi} \tilde{y}_{ij}^L) L_{R,j} + \bar{Q}_{L,i} (\phi y_{ij}^Q + \tilde{\phi} \tilde{y}_{ij}^Q) Q_{R,j} \\
 & + \bar{L}_{R,i} \tilde{\chi}_R y_{ij}^S S_{2,j}^C + H.c. . \tag{2}
 \end{aligned}$$

- Spontaneous symmetry breaking (SSB) occurs via the vevs

$$\langle \phi \rangle = \begin{pmatrix} k_1 & 0 \\ 0 & k_2 \end{pmatrix} \sim \mathcal{O}(\text{GeV}), \quad \langle \chi \rangle = \begin{pmatrix} 0 \\ v_R \end{pmatrix} \sim \mathcal{O}(\text{TeV}). \quad (3)$$

and $t_\beta = \tan \beta = k_1/k_2$, $v = \sqrt{k_1^2 + k_2^2} = 246 \text{ GeV}$.

- After SSB, the IS neutrino masses Lagrangian is [16, 17, 12, 18]

$$\mathcal{L}_m^\nu = M_D \bar{\nu}_L \nu_R + M_R \bar{\nu}_R^c S_2 + \mu_s \bar{S}_2^c S_2 + h.c., \quad (4)$$

where $M_D = v(y^L s_\beta + \tilde{y}^L c_\beta)/\sqrt{2}$ is the neutrino Dirac mass matrix and $M_R = y^s v_R/\sqrt{2}$.

- In the basis (ν_L^c, ν_R, S_2) , the neutrino mass matrix is

$$\mathcal{M}_\nu = \begin{pmatrix} 0 & M_D & 0 \\ M_D^T & 0 & M_R \\ 0 & M_R^T & \mu_s \end{pmatrix}. \quad (5)$$

- The physical light and heavy neutrino states ν_{ℓ_i}, ν_{h_j} , have masses

$$m_{\nu_{\ell_i}} = M_D M_R^{-1} \mu_s (M_R^T)^{-1} M_D^T, \quad i = 1 \dots 3, \quad (6)$$

$$m_{\nu_{h_j}}^2 = M_R^2 + M_D^2, \quad j = 1 \dots 6. \quad (7)$$

- The inverse relation of Eq. (6) is

$$M_D = U_{\text{PMNS}} \sqrt{m_{\nu_\ell}} \mathcal{R} \sqrt{(\mu^s)^{-1}} M_R, \quad (8)$$

\mathcal{R} is an orthogonal matrix and U_{PMNS} is the 3×3 light neutrino mixing [7, 1, 9].

- Choices of $\mu_s \sim \mathcal{O}(10^{-7})$ GeV, and $v_R \sim \mathcal{O}(10^3)$ GeV So for $y^s \sim \mathcal{O}(10^{-3})$ we need $M \sim \mathcal{O}(10)$ TeV gives the experimental light neutrino masses.

- The symmetric mass matrix of the charged Higgs bosons $(\phi_1^\pm, \phi_2^\pm, \chi_R^\pm)$ is

$$M_{H^\pm}^2 = \frac{\alpha_{32}}{2} \begin{pmatrix} \frac{v_R^2 s_\beta^2}{c_{2\beta}} & \frac{v_R^2 s_{2\beta}}{2c_{2\beta}} & -vv_R s_\beta \\ \cdot & \frac{v_R^2 c_\beta^2}{c_{2\beta}} & -vv_R c_\beta \\ \cdot & \cdot & v^2 c_{2\beta} \end{pmatrix}, \quad (9)$$

- Only one physical charged Higgs boson with mass are

$$m_{H^\pm}^2 = \frac{\alpha_{32}}{2} \left(\frac{v_R^2}{c_{2\beta}} + v^2 c_{2\beta} \right), \quad (10)$$

where $\alpha_{32} = \alpha_3 - \alpha_2$.

- For $v_R \gtrsim \mathcal{O}(\text{TeV})$, the physical charged Higgs boson is [10]

$$H^\pm \approx -(s_\beta \phi_1^\pm + c_\beta \phi_2^\pm). \quad (11)$$

- The relevant H^\pm -fermions couplings are

$$\Gamma_{\bar{u}_i d_j}^{H^\pm} = C_{ij} P_L + D_{ij} P_R, \quad \Gamma_{\bar{\nu}_k \ell}^{H^\pm} = \xi_{kl} P_L + \zeta_{kl} P_R. \quad (12)$$

and the couplings

$$C_{ij} \simeq \frac{\sqrt{2}}{v c_{2\beta}} \sum_{a=1}^3 V_{ja}^* (V M_d V^\dagger - s_{2\beta} M_u)_{ai}^*, \quad (13)$$

$$D_{ij} \simeq \frac{\sqrt{2}}{v c_{2\beta}} \sum_{a=1}^3 V_{ja} (s_{2\beta} V M_d V^\dagger - M_u)_{ia}, \quad (14)$$

$$\xi_{kl} \simeq \frac{\sqrt{2}}{v c_{2\beta}} \sum_{i=1}^3 U_{k,i+3}^* (s_{2\beta} M_{\text{lp}} - M_D)_{li}, \quad k = 4, \dots, 9, \quad (15)$$

$$\zeta_{kl} \simeq \frac{\sqrt{2}}{v c_{2\beta}} \sum_{i=1}^3 U_{ki} (M_{\text{lp}} - s_{2\beta} M_D)_{il}, \quad k = 1, 2, 3, \quad (16)$$

V and U are the quark CKM and IS neutrino mixing matrices.

Outline

1 The LRIS Model

2 a_μ in LRIS

3 LFV Constraints

4 Conclusion

- Recent experimental results indicate a possible 4.2σ difference between the measured value of the anomalous magnetic moments of muons a_μ and the SM expectations [11, 14, 13, 2], namely

$$\delta a_\mu = a_\mu^{\text{exp}} - a_\mu^{\text{SM}} = (2.51 \pm 0.59) \times 10^{-9}. \quad (17)$$

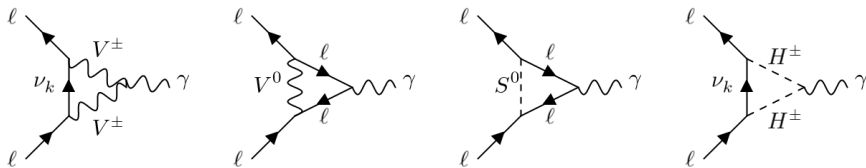


Figure 1: LRIS one-loop Feynman diagrams contributions to lepton $g_l - 2$ via massive neutrinos, $V^\pm = W, W'$, $V^0 = Z, Z'$, $S^0 = h, A$ and the charged Higgs boson H^\pm .

- The charged Higgs H^\pm contribution to a_μ is given by

$$a_\ell^{H^\pm} = G_F^\ell \Gamma_\gamma^{H^\pm} \sum_{k=1}^9 \left(|\zeta'_{k\ell}|^2 \mathcal{F}_2(x_{H^\pm}^{\nu_k}) + 2\text{Re}[\zeta'_{k\ell} \xi'_{k\ell}^*] \mathcal{F}_1(x_{H^\pm}^{\nu_k}) \right), \quad (18)$$

where the couplings $\zeta'_{k\ell} = \frac{v}{m_{\nu_k}} \zeta_{k\ell}$ and $\xi'_{k\ell} = \frac{v}{m_\ell} \xi_{k\ell}$.

- The charged Higgs boson interaction coupling with photons is

$$\Gamma_\gamma^{H^\pm} \simeq \frac{1}{6e} \left(g_L U_{21}^0 + g_R U_{31}^0 \right), \quad (19)$$

U^0 is the neutral gauge bosons mixing [10].

- The loop functions \mathcal{F}_k ($k = 1, 2$) in Eq. (18) are given by

$$\mathcal{F}_k(y) = \frac{y \mathcal{P}_k(y)}{(y-1)^{k+1}} - \frac{6y^{k+1} \log(y)}{(y-1)^{k+2}}, \quad k = 1, 2, \quad (20)$$

$$\mathcal{P}_1(y) = 3y + 3, \quad (21)$$

$$\mathcal{P}_2(y) = 2y^2 + 5y - 1. \quad (22)$$

- The charged Higgs boson contribution to the a_μ anomaly Eq. (18) can be approximated to

$$a_\ell^{H^\pm} \simeq 2G_F^\ell \Gamma_\gamma^{H^\pm} \sum_{k=4}^9 \text{Re}[\zeta'_{k\ell} \xi'_{k\ell}^*] \mathcal{F}_1(x_{H^\pm}^{\nu_k}) \simeq \frac{3\Gamma_\gamma^{H^\pm}}{8\pi^2} m_\ell \sum_{k=4}^9 \frac{\zeta_{k\ell} \xi_{k\ell}}{m_{\nu_k}}. \quad (23)$$

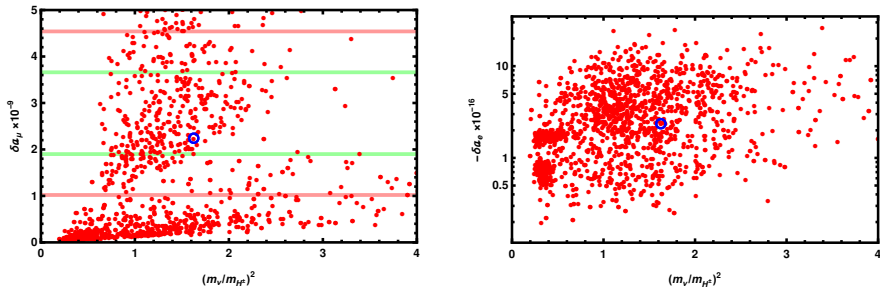


Figure 2: (Left/right) $\delta a_{\mu,e}$ with $x_{H^\pm}^{\nu_5} = m_{\nu_5}^2/m_{H^\pm}^2$. The 1σ and 2σ standard errors of measurements of a_μ are included in green and red borders. BP is encircled.

α_{32}	t_β	v_R	$Z_{31}^{H^\pm}$	$Z_{32}^{H^\pm}$	$Z_{33}^{H^\pm}$	m_{H^\pm}
0.0058	0.1	10000	-0.099	-0.994	0.024	545

Table 2: BP and H^\pm mixing and mass for

$y^s = \text{diag}(1.53 \times 10^{-2}, 9.76 \times 10^{-1}, 2.05 \times 10^{-1})$ and

$\mu^s = \text{diag}(1.01 \times 10^{-5}, 3.82 \times 10^{-9}, 5.49 \times 10^{-6})$. Finally, the nonvanishing elements of the orthogonal matrix \mathcal{R} are $\mathcal{R}_{13} = \mathcal{R}_{21} = \mathcal{R}_{32} = 1$.

m_{ν_1}	m_{ν_2}	m_{ν_3}	m_{ν_4}	m_{ν_5}	m_{ν_6}	m_{ν_7}	m_{ν_8}	m_{ν_9}
1.0×10^{-13}	8.5×10^{-12}	5.0×10^{-11}	108	695	1449	108	695	1449

Table 3: BP neutrino mass spectrum in GeVs.

δa_μ	$-\delta a_e$	$\text{BR}(\mu \rightarrow e\gamma)$
2.5×10^{-9}	8.1×10^{-17}	3.4×10^{-13}

Table 4: BP Observables $g_{\mu(e)} - 2$, $\text{BR}(\mu \rightarrow e\gamma)$ of the BP given in Tab. 3.

Outline

1 The LRIS Model

2 a_μ in LRIS

3 LFV Constraints

4 Conclusion

- Experimentally, $\text{BR}(\mu \rightarrow e\gamma) \lesssim 4.2 \times 10^{-13}$ (90%CL) [5]. LRIS H^\pm

$$\begin{aligned} \text{BR}(\mu \rightarrow e\gamma)_{\text{LRIS}} &\simeq \frac{\alpha_w^3 s_w^2}{256\pi^2} \frac{m_\mu}{\Gamma_\mu} (x_W^\mu)^2 \sum_{k=4}^9 \left| (\zeta'_{k,e} \xi'_{k,\mu} + \xi'_{k,e} \zeta'_{k,\mu}) \mathcal{F}_1(x_{H^\pm}^{\nu_k}) \right|^2 \\ &\lesssim \frac{9\alpha_{\text{em}}}{256\pi^4} \frac{m_\mu^5}{\Gamma_\mu} \sum_{k=4}^9 \frac{1}{m_{\nu_k}^2} \left(\frac{\zeta_{k,e} \xi_{k,\mu}}{m_\mu} + \frac{\xi_{k,e} \zeta_{k,\mu}}{m_e} \right)^2. \end{aligned} \quad (24)$$

- Finally, we check experimental limits on H^\pm contributions to the μ - e conversion on a nucleus (A). Experiments make the upper bounds $R_{\mu \rightarrow e}^{\text{Ti}} \leq 10^{-18}$, $R_{\mu \rightarrow e}^{\text{Al}} \leq 10^{-16}$, $R_{\mu \rightarrow e}^{\text{Au}} \leq 7 \times 10^{-13}$ [15].
- The H^\pm contribution to the μ - e conversion is [3, 8]

$$R_{\mu \rightarrow e}^A = \frac{32G_F^2 m_\mu^5}{\Gamma_{\text{capt}}^A} \left[\left| \tilde{C}_{V,R}^{pp} V_A^{(p)} + \tilde{C}_{V,R}^{nn} V_A^{(n)} + \frac{1}{4} C_{D,L} D_A \right|^2 + \{L \leftrightarrow R\} \right]. \quad (25)$$

$\Gamma_{\text{capt}}^A \sim \mathcal{O}(1 - 10) \times 10^6 \text{ s}^{-1}$ is the rate for the muon to transform to a neutrino by capture on the nucleus (A). The nuclear “overlap integrals” $V_A^{(p)}, V_A^{(n)}, D_A \sim \mathcal{O}(10^{-2} - 10^{-1})$ for $A = \text{Al, Ti, Au}$ [15].

- In LRIS, the nucleon-dependent Wilson coefficients are given by

$$C_{D,L} = \frac{8G_F\alpha_{em}}{\pi s_w^2\sqrt{2}} \sum_{k=1}^9 \sum_{j=1}^3 \sum_{q,q'=u,d,q\neq q'} (U_{k,e}^* U_{k,\mu} |V_{q',q_j}|^2) B_2(x_W^{\nu_k}, x_W^{q_j}), \quad (26)$$

$$\begin{aligned} \tilde{C}_{V,R}^{pp} &= \frac{1}{8\pi^2 m_{H^\pm}^2} \sum_{k=1}^9 \sum_{j=1}^3 \sum_{q,q'=u,d,q\neq q'} (\zeta_{k,e}\xi_{k,\mu} + \zeta_{k,\mu}\xi_{k,e}) \\ &\times (C_{q',q_j}^2 + D_{q',q_j}^2) B_2(x_{H^\pm}^{\nu_k}, x_{H^\pm}^{q_j}), \end{aligned} \quad (27)$$

$$\begin{aligned} \tilde{C}_{V,R}^{nn} &= \frac{1}{4\pi^2 m_{H^\pm}^2} \sum_{k=1}^9 \sum_{j=1}^3 \sum_{q,q'=u,d,q\neq q'} (\zeta_{k,e}\zeta_{k,\mu} + \xi_{k,e}\xi_{k,\mu}) \\ &\times (C_{q',q_j} D_{q',q_j}) B_1(x_{H^\pm}^{\nu_k}, x_{H^\pm}^{q_j}) \sqrt{x_{H^\pm}^{\nu_k} x_{H^\pm}^{q_j}}, \end{aligned} \quad (28)$$

- The loop functions are

$$J_k(x) = \frac{1}{1-x} + \frac{x^k \log(x)}{(1-x)^2}, \quad (29)$$

$$B_k(x, y) = \frac{J_k(x) - J_k(y)}{x - y}, \quad k = 1, 2. \quad (30)$$

$\text{BR}(\mu \rightarrow e\gamma)$	$R_{\mu \rightarrow e}^{\text{Al}}$	$R_{\mu \rightarrow e}^{\text{Ti}}$	$R_{\mu \rightarrow e}^{\text{Au}}$
2.10×10^{-13}	4.10×10^{-51}	3.80×10^{-50}	4.10×10^{-49}

Table 5: LFV observables BP given in Table 3 in LRIS.

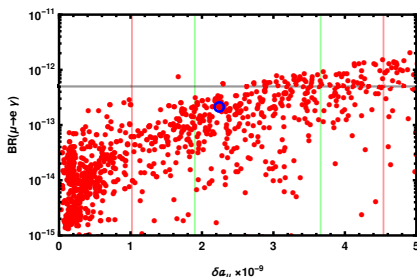


Figure 3: $\text{BR}(\mu \rightarrow e\gamma)$ versus δa_μ in LRIS. BP is encircled.

- All BPs are tested and found to satisfy the μ - e conversion experimental limits as in Table 5.

Outline

1 The LRIS Model

2 a_μ in LRIS

3 LFV Constraints

4 Conclusion

- We have analyzed a_μ in a minimal left-right symmetric model with an inverse seesaw mechanism.
- We found that a large region of the parameter space of the model is consistent with the observed a_μ anomaly.
- BP satisfy the δa_e limits and the $\text{BR}(\mu \rightarrow e\gamma)$ and the $\mu \rightarrow e$ -conversion rates limits.

References I

- [1] W. Abdallah, A. Awad, S. Khalil, and H. Okada.
Muon Anomalous Magnetic Moment and $\mu \rightarrow e \gamma$ in B-L Model with Inverse Seesaw.
[Eur. Phys. J. C, 72:2108, 2012.](#)
- [2] B. Abi et al.
Measurement of the Positive Muon Anomalous Magnetic Moment to 0.46 ppm.
[Phys. Rev. Lett., 126\(14\):141801, 2021.](#)
- [3] R. Alonso, M. Dhen, M. B. Gavela, and T. Hambye.
Muon conversion to electron in nuclei in type-I seesaw models.
[JHEP, 01:118, 2013.](#)
- [4] M. Ashry, K. Ezzat, and S. Khalil.
Muon $g-2$ anomaly in a left-right model with an inverse seesaw mechanism.
[Phys. Rev. D, 107\(5\):055044, 2023.](#)
- [5] A. M. Baldini et al.
Search for the lepton flavour violating decay $\mu^+ \rightarrow e^+ \gamma$ with the full dataset of the MEG experiment.
[Eur. Phys. J. C, 76\(8\):434, 2016.](#)
- [6] Debasish Borah, Sudhanwa Patra, and Utpal Sarkar.
TeV scale Left Right Symmetry with spontaneous D-parity breaking.
[Phys.Rev., D83:035007, 2011.](#)
- [7] J.A. Casas and A. Ibarra.
Oscillating neutrinos and $\mu \rightarrow e, \gamma$.
[Nuclear Physics B, 618\(1\):171–204, 2001.](#)

References II

- [8] Sacha Davidson, Yoshitaka Kuno, and Masato Yamanaka.
Selecting $\mu \rightarrow e$ conversion targets to distinguish lepton flavour-changing operators.
[Phys. Lett. B](#), 790:380–388, 2019.
- [9] Ivan Esteban, M. C. Gonzalez-Garcia, Michele Maltoni, Thomas Schwetz, and Albert Zhou.
The fate of hints: updated global analysis of three-flavor neutrino oscillations.
[JHEP](#), 09:178, 2020.
- [10] K. Ezzat, M. Ashry, and S. Khalil.
Search for a heavy neutral Higgs boson in a left-right model with an inverse seesaw mechanism at the LHC.
[Phys. Rev. D](#), 104(1):015016, 2021.
- [11] F. J. M. Farley, K. Jungmann, J. P. Miller, W. M. Morse, Y. F. Orlov, B. L. Roberts, Y. K. Semertzidis, A. Silenko, and E. J. Stephenson.
A New method of measuring electric dipole moments in storage rings.
[Phys. Rev. Lett.](#), 93:052001, 2004.
- [12] M.C. Gonzalez-Garcia and J.W.F. Valle.
Fast Decaying Neutrinos and Observable Flavor Violation in a New Class of Majoron Models.
[Phys. Lett. B](#), 216:360–366, 1989.
- [13] Alexander Keshavarzi, William J. Marciano, Massimo Passera, and Alberto Sirlin.
Muon $g - 2$ and $\Delta\alpha$ connection.
[Phys. Rev. D](#), 102(3):033002, 2020.
- [14] On Kim et al.
Reduction of coherent betatron oscillations in a muon $g - 2$ storage ring experiment using RF fields.
[New J. Phys.](#), 22(6):063002, 2020.

References III

- [15] [Ryuichiro Kitano, Masafumi Koike, and Yasuhiro Okada.](#)
Detailed calculation of lepton flavor violating muon electron conversion rate for various nuclei.
[Phys. Rev. D](#), 66:096002, 2002.
[Erratum: [Phys.Rev.D](#) 76, 059902 (2007)].
- [16] [R.N. Mohapatra.](#)
Mechanism for Understanding Small Neutrino Mass in Superstring Theories.
[Phys. Rev. Lett.](#), 56:561–563, 1986.
- [17] [R.N. Mohapatra and J.W.F. Valle.](#)
Neutrino Mass and Baryon Number Nonconservation in Superstring Models.
[Phys. Rev. D](#), 34:1642, 1986.
- [18] [C. Weiland.](#)
Enhanced lepton flavour violation in the supersymmetric inverse seesaw.
[J. Phys. Conf. Ser.](#), 447:012037, 2013.

Thank you!
Questions?